

6th Historic Mortars Conference

21st to 23rd September 2022
Ljubljana, Slovenia

CONFERENCE PROCEEDINGS



Proceedings of the 6th Historic Mortars Conference - HMC 2022
21-23 September 2022, University of Ljubljana, Ljubljana, Slovenia

Edited by
Violeta Bokan Bosiljkov
Andreja Padovnik
Tilen Turk
Petra Štukovnik

CIP - Kataložni zapis o publikaciji
Narodna in univerzitetna knjižnica, Ljubljana

691.53(082)(0.034.2)

HISTORIC Mortars Conference (6 ; 2022 ; Ljubljana)

6th Historic Mortars Conference [Elektronski vir] : 21st to 23rd September 2022, Ljubljana, Slovenia : conference proceedings / [edited by Violeta Bokan Bosiljkov ... et al.]. - Ljubljana : Faculty of Civil and Geodetic Engineering, 2022

ISBN 978-961-6884-77-8
COBISS.SI-ID 121348355

An investigation of the salt weathering resistance of heritage repair mortar mixes	525
Anupama V.A., Divya Rani S., Swathy Manohar and Manu Santhanam	
Design rationale and field testing of a gypsum-based grout for wall painting stabilization in the Chapel of Niketas the Stylite, Cappadocia, Turkey	534
Jennifer Herrick Porter, Yoko Taniguchi and Hatice Temur Yildiz	
Comparative evaluation of properties of laboratory test specimens for masonry mortars prepared using different compaction methods	550
Vadim Grigorjev, Miguel Azenha and Nele De Belie	
The challenge on development of the repair mortars for historical buildings in severe marine environment: Paimogo Fort, a case study	563
Maria do Rosário Veiga and Ana Rita Santos	
Practical test for pozzolanic properties by A. D. Cowper: implementation and innovation	578
Marlene Sámano Chong, Alberto Muciño Vélez, Ivonne Rosales Chávez and Luis Fernando Guerrero Baca	
Determination of the salt distribution in the lime-based mortar samples using XRF and SEM – EDX characterisation	595
Marina Aškričić, Dimitrije Zakić, Aleksandar Savić, Ljiljana Miličić, Ivana Delić-Nikolić and Martin Vyšvařil	
Developing a lime-based injection grout with no additives for very thin delamination: the role of aggregates and particle size/morphology	607
Chiara Pasian, Jennifer H. Porter, Mariia Gorodetska and Stephanie Parisi	
Enhancement of latent heat storage capacity of lime rendering mortars	620
Andrea Rubio-Aguinaga, José María Fernández, Íñigo Navarro-Blasco and José Ignacio Álvarez	
Obtaining of repair lime renders with microencapsulated phase change materials: optimization of the composition, application, mechanical and microstructural studies	634
Andrea Rubio-Aguinaga, José María Fernández, Íñigo Navarro-Blasco and José Ignacio Álvarez	
Time-dependent deformations of lime-based mortars and masonry specimens prepared with them	649
Ioanna Papayianni and Emmanuella Berberidou	
Influence of methyl cellulose in injection grout on mould growth on mural paintings - preliminary results	657
Andreja Padovnik, Violeta Bokan Bosiljkov, Polonca Ropret and Janez Kosel	

ENHANCEMENT OF LATENT HEAT STORAGE CAPACITY OF LIME RENDERING MORTARS

Andrea Rubio-Aguinaga¹, José María Fernández¹, Íñigo Navarro-Blasco¹ and José Ignacio Álvarez¹

(1) University of Navarra, Pamplona, Spain

Abstract: Microencapsulated Phase Change Materials (PCMs) were included in air lime rendering mortars in order to improve the thermal comfort of the inhabitants and the energy efficiency of buildings of the Architectural Heritage under the premises of minimum intervention and maximum compatibility. Three different PCMs were tested and directly added during the mixing process to fresh air lime mortars in three different percentages: 5, 10 and 20 wt. %. Some chemical additives were also incorporated to improve the final performance of the renders: a starch derivative as an adhesion booster; metakaolin as pozzolanic addition to shorten the setting time and to increase the final strength; and a polycarboxylated ether as a superplasticizer to adjust the fluidity of the fresh renders avoiding an excess of mixing water. The specific heat C_p , the enthalpy ΔH ascribed to the phase change and the melting temperature of the PCMs were determined by Differential Scanning Calorimetry (DSC). The capacity of the renders to store/release heat was demonstrated at a laboratory scale. The favourable results proved the effect of these PCMs with respect to the thermal performance of these rendering mortars, offering a promising way of enhancement of the thermal efficiency of building materials of the Cultural Heritage.

1 Introduction

One of the goals of today's society, with greater concern for the environment and sustainability, is to reduce global energy consumption. According to the International Energy Agency (IEA), the construction sector is one of the largest consumers of energy due to the energy costs associated with heating and cooling buildings [1]. For this reason, in recent years, thermal energy storage (TES) systems have been extensively studied in order to improve the thermal efficiency of buildings, with Phase Change Materials (PCM) standing out in particular [1].

Phase change materials are systems capable of storing latent thermal energy through phase changes. Generally, these phase changes are solidification and melting. Thus, during the melting process, the heat gain is stored in the form of latent heat of fusion and, during the solidification process; this latent heat is released [2]. Therefore, depending on the external temperature of the system, heat is released or absorbed regulating moderately the temperature of the medium [1].

Phase change materials are a family of materials with high heat values of melting and solidification with the ability to absorb or release large amounts of thermal energy at constant temperature (latent heat) when subjected to a phase change [3]. The characteristics required for a material to be considered a PCM are: non-corrosive, non-toxic, inert, high latent heat, high thermal conductivity, low-priced, congruent melting and not undergo (or at least minimally) subcooling [4]. Phase change materials can be classified according to different criteria. A

distinction is made between liquid-liquid PCMs and solid-liquid PCMs according to the state transition. The latter are the most commonly used because of the higher enthalpy associated with the phase change due to the greater freedom of movement of the molecules in the liquid state with respect to those in the solid state [3]. At the same time, solid-liquid PCMs are classified according to their composition as: inorganic (hydrated salts, molten salts and eutectic salts), organic (fatty acids, sugars, crystalline polymers and paraffin waxes) and metallic (metals and alloys) [3,4].

Ancient monuments or traditional residential buildings show low levels of thermal efficiency and when repair works are addressed the enhancement of the thermal comfort conditions and the reduction of energy consumption is required. There are numerous strategies for the reduction of the thermal demand; however, most of the available envelope upgrades cannot be applied in repair works of Cultural Heritage buildings. This is because their application, their high price, and their incompatibility with some architectural heritage structures do not meet the general requirements of recognition of the tangible and intangible values of Cultural Heritage as well as the performance standards for protection and restoration, such as minimal modification of the aesthetic and history of the property, minimal intervention, highest compatibility of the materials to be introduced and use of new materials and methods for restoration and conservation. For this reason, the incorporation of PCMs in lime renders is, apparently, a suitable option for enhancement the thermal efficiency of historic buildings and monuments as it respects all the above mentioned requirements. However, there is little literature available on the incorporation of phase change materials into lime-based mortars.

There are different methods for the incorporation of PCMs in building materials, the most important are: direct incorporation (mixed directly with the building material), direct immersion (immersion of the porous building material into the molten PCMs), macroencapsulation (panels, tubes and spheres filled with large amounts of PCMs), microencapsulation (PCMs with sizes between 0.1 μm and 1 mm that are enclosed in microcapsules), shape stabilization (melting and mixing of PCM with a polymeric support material), and form-stable method (PCM entrapped in porous polymeric matrix) [1]. In the present work, solid-liquid PCMs are used, whose main drawback is the volume variations they undergo during phase changes that can lead to diffusion of the PCMs in the composite and cause microstructural changes and leakage [3-5]. Therefore, microencapsulated PCMs are used so the macroscopic shape of the PCM is maintained, the heat transfer area is increased and undesired movements in the matrix are avoided, in addition to meeting the restoration and conservation criteria [3].

Paraffin is one of the most studied and widely used solid-liquid PCMs [4]. Paraffin waxes are mainly composed of mixtures of linear alkanes (around 75-100%) together with a small percentage of branched alkanes (isoalkanes, cycloalkanes, alkylbenzenes...) [2]. Commercial paraffin waxes are inexpensive, have a wide range of melting temperatures, have a high latent heat, are thermally and chemically stable, are non-toxic and do not undergo subcooling (4,5). However, the application of paraffin waxes as PCMs is limited by their low thermal conductivity ($\sim 0.2 \text{ W/m K}$) which causes a reduction of their rates of heat storage and release during melting and solidification [4,5]. Consequently, microencapsulation is normally used in order to enhance thermal conductivity by maximizing their heat transfer area.

The aim of this work is the incorporation of microencapsulated PCMs in lime mortars in order to improve the energy efficiency and thermal comfort of the buildings of the architectural heritage.

The selection of PCMs for its application as thermal energy storage systems was carried out according to the melting temperature. Specifically, in this work microencapsulated paraffin and bio-based PCMs were assayed. Melting temperatures were selected in order to storage/release heat under rather cold climate conditions ($T_{\text{melting}} \sim 18\text{ }^{\circ}\text{C}$) or hot climates ($T_{\text{melting}} \sim 25\text{ }^{\circ}\text{C}$). This way, the incorporation of these PCMs in lime mortars will be able to reduce the differences between peak and off-peak thermal loads, reduction of energy consumption, cut in electricity demand, indoor thermal comfort improvement and, ultimately, reduction of CO₂ release to the atmosphere.

In this work, percentages of 5, 10 and 20 wt. % of three different microencapsulated PCMs were added during the mixing process to fresh air lime mortars. The PCMs used were two paraffin-based PCMs with melamine microcapsule with melting points of 18°C and 24°C and a bio-based microencapsulated PCM with melting temperature of 29°C. Other chemical additives were also incorporated to improve the final performance of the renders: a starch derivative as an adhesion booster, metakaolin as pozzolanic addition to shorten the setting time and to increase the final strength; and a polycarboxylate ether as a superplasticizer to adjust the fluidity of the fresh renders avoiding an excess of mixing water.

2 Materials and methods

2.1 Materials

Rendering air lime mortars were prepared by mixing calcitic air lime supplied by Cal Industrial S.A. (Calinsa Navarra), classified as CL-90-S by European regulations and calcitic sand (supplied by CTH Navarra). Percentages of binder/aggregate weight ratio were 21.7/78.3, whereas the percentage of mixing water was fixed at 25 wt. % of the total weight of the mortar.

To obtain easily workable renders with good performance, different additives and mineral admixtures were also used to optimize the mix composition. A superplasticizer (polycarboxylated ether derivative, MasterCast GT 205) was added to adjust the fluidity of the fresh renders avoiding an excess of mixing water. Different percentages of a starch derivative (Casaplast) were added as an adhesion booster. Metakaolin (MK, supplied by METAVER) was added in some of the mortars (20 wt. % with respect to the weight of lime, bwol) in order to increase the final strength and durability of the rendering mortars.

Three different solid-liquid microencapsulated PCMs supplied by Microtek, were used: two paraffin-based PCMs with melamine microcapsule with melting points of 18°C and 24°C (denoted as 18PCM and 24PCM) and a bio-based microencapsulated PCM with melting temperature of 29°C (29PCM). Percentages bwol of 5%, 10% and 20% of PCM were directly added to fresh air lime mortars during the mixing process.

As control group two PCM-free mortars (CTRL-1, MK-free, and CTRL-2, with 20 wt.% of MK) were prepared in order to compare the PCM performance (Table 1 and Table 2 gather the composition of the mixes).

The consistency of all the samples was assessed by the flow table test and seen to be within the range of 160-215 mm of slump.

Table 1. Composition of PCM-free renders and renders containing 24PCM and their fluidity and adhesion test.

Render	PCM-free		24PCM					
	CTRL-1	CTRL-2	24PCM-1	24PCM-2	24PCM-3	24PCM-4	24PCM-5	24PCM-6
PCM (wt. %)	0	0	5	5	10	10	20	20
SP (wt. %)	0.6	0.75	0.75	0.75	0.75	0.75	0.75	0.75
MK (wt. %)	0	20	0	20	0	20	0	20
Starch (wt. %)	0.50	0.50	0.50	0.50	0.50	0.50	0.50	0.50

Table 2. Composition of renders containing 18PCM and their fluidity and adhesion test.

Render	18PCM					
	18PCM-1	18PCM-2	18PCM-3	18PCM-4	18PCM-5	18PCM-6
PCM (wt. %)	5	5	10	10	20	20
SP (wt. %)	0.75	0.75	0.75	0.75	0.75	0.75
MK (wt. %)	0	20	0	20	0	20
Starch (wt. %)	0.50	0.50	0.50	0.50	0.50	0.50

Table 3. Composition of renders containing 29PCM and their fluidity and adhesion test.

Render	29PCM					
	29PCM-1	29PCM-2	29PCM-3	29PCM-4	29PCM-5	29PCM-6
PCM (wt. %)	5	5	10	10	20	20
SP (wt. %)	0.75	0.75	0.75	0.75	0.75	0.75
MK (wt. %)	0	20	0	20	0	20
Starch (wt. %)	0.50	0.50	0.50	0.50	0.50	0.50

2.2 Experimental methods

For the preparation of the fresh grouts, air lime, sand, metakaolin, adhesion booster, the corresponding PCM and an initial percentage of superplasticizer (0.25% with respect to the weight of lime, bwol) were blended for 5 min using a solid additives mixer BL-8-CA (Lleal, S.A., Granollers, Spain) to achieve a homogenous mix.

A fixed percentage of mixing water (25 wt. %) was then added at low speed for 270 s in a Proeti ETI 26.0072 (Proeti, Madrid, Spain) mixer. Accumulative additions of 0.25% bwol of superplasticizer were added until adequate fluidity (as measured by the flow table test). For each render, the percentages of SP (along with the adhesion booster) were modified until applicable, adherent and low-cracking renders were achieved, as detailed in a further work.

Regarding the hardened state study, fresh mixtures were moulded into cylindrical specimens with dimensions of 33 mm diameter and 39 mm height, and then cured at lab conditions (20°C ± 0.5 °C and 45% ± 5% RH).

2.3 Characterization methods

The characterization and study of the thermal properties of the mortars was carried out through different techniques, such as Thermogravimetric Analysis (TGA), Differential Scanning Calorimetry (DSC) and thermal conductivity measurements.

2.3.1 DSC

Thermal performance of the enhanced lime-based mortars was studied by Differential Scanning Calorimetry (DSC). The parameters studied were specific heat capacity (C_p), the enthalpy (ΔH_m) ascribed to the phase change and the melting temperature (T_m) of the PCMs, i.e., the latent heat storage.

The equipment used to perform the DSC analysis was the DSC25 TA Instruments and the data evaluation was carried out with TRIOS from TA Instruments. C_p was determined using modulated DSC in a range of temperatures of -25°C to 60°C . ΔH_m and T_m were determined in powdered representative samples of ca. 7 mg, in 40 μL aluminium pans with hermetic lids, applying 3 cycles of heating-cooling between 0°C and 50°C with an increment of $5^\circ\text{C}/\text{min}$. At the beginning and end of each cycle an isotherm is applied for 5 minutes. All analyses are performed under nitrogen atmosphere (flow of 50 mL/min).

2.3.2 TGA

Thermogravimetric analysis was used to study the thermal stability of the renders. The equipment used to perform the thermogravimetric analysis was the SDTA650 TA Instruments and the data evaluation was carried out with TRIOS from TA Instruments. Samples of ca. 10 mg in 90 μL alumina pans were analysed. The heating program applied consisted of a heating ramp ($20^\circ\text{C}/\text{min}$) from 35°C to 1000°C under a nitrogen atmosphere (flow of 100 mL/min).

2.3.3 Thermal conductivity measurements

The equipment used to perform the thermal conductivity measurements was the FOX50 Heat Flow Meter from TA Instruments. This instrument consists of two parallel plates controlled by two independent Peltier cells. Each plate is subjected to a specific temperature with a temperature difference between plates of 10°C , thus generating a thermal gradient and obtaining the thermal conductivity at the average temperature between the two plates. Strict thermal equilibrium criteria were applied to the measurements consisting of 6 consecutive blocks of data acquisition. These criteria included, for each plate, a temperature deviation of less than 1°C from the setpoint temperature and a variation of less than 200 μV of the transducer signals from those obtained in the previous block.

The thermal conductivity of 55 mm diameter and 20 mm thick disks of the rendering mortars was measured at 5°C , 15°C , 25°C and 35°C . In this way, the conductivity of the macroscopic material is measured at temperatures where the PCM is in the solid state and in the liquid state. In all cases, renders were, at least, 28 days cured before the thermal conductivity measurement. In addition, in order to obtain more representative values three disks of each render were measured and the average was calculated along with its standard deviation.

3 Results and discussion

3.1 Evaluation of latent heat thermal energy storage

Firstly, pure microencapsulated PCMs thermal stabilities were analysed by TGA (Figure 1). The degradation of the additive is observed in all cases at around 400 °C typical of melamine [8]. It is notable in the case of 24PCM that it starts to degrade at lower temperatures with a smaller mass loss at 155°C.

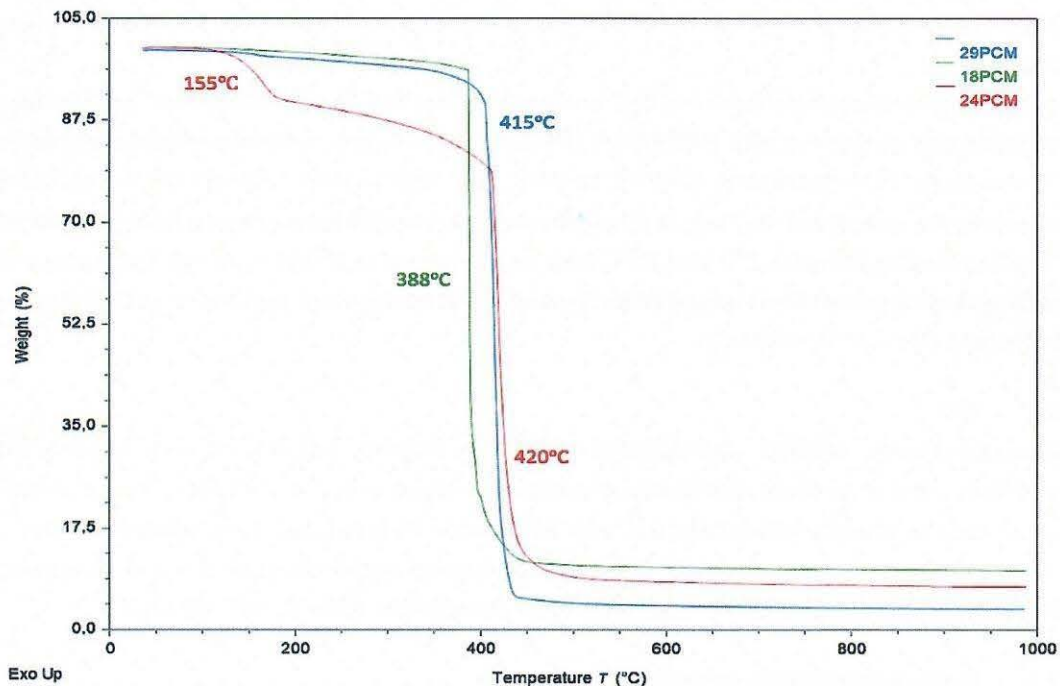


Figure 1. TGA curves of pure PCMs.

The thermal stabilities of PCM-bearing renders were also studied. Figure 2 includes TGA curves of some PCM-bearing renders in comparison with the PCM-free render (CTRL-1). It is shown in all cases the degradation of the PCM around 400 °C and the calcite decarbonation at 800 °C [9].

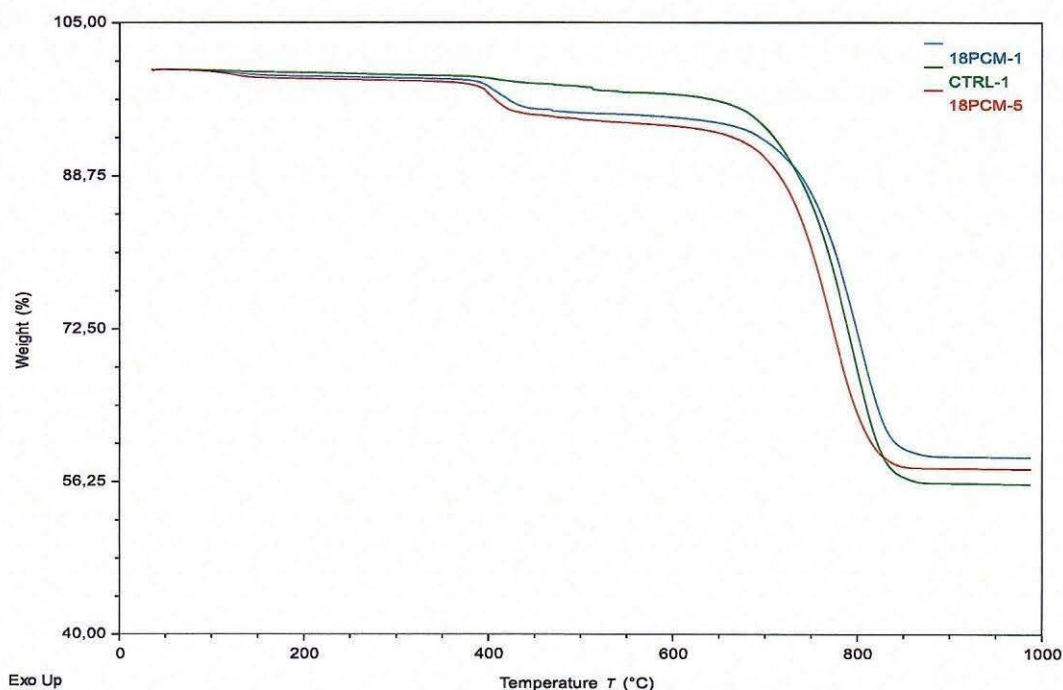


Figure 2. TGA curves of 18PCM-1, 18PCM-5 and CTRL-1.

The parameters obtained with the DSC measurements were the melting temperature (T_m), the enthalpy ascribed to the phase change (ΔH_m) (that is, the latent heat thermal energy storage capacity) and the specific heat capacity (C_p). These parameters are useful for the study of the thermal behaviour of mortars after the addition of different percentages of PCMs.

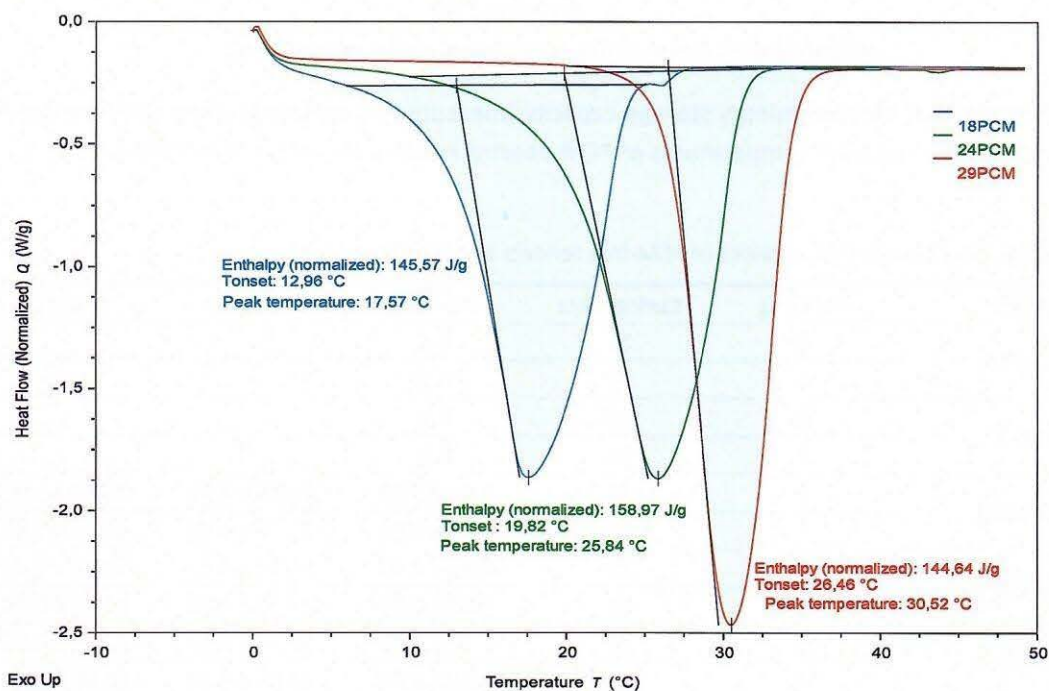


Figure 3. DSC curves of pure PCMs.

Pure PCMs were studied. Figure 3 depicts the heat flows during the melting processes of the pure PCMs. It can be seen how all of them present similar enthalpies around 150 J/g, the highest (158.97 J/g) corresponding to the 24PCM additive. In addition, it is possible to check that their melting temperatures are in accordance with their data sheets.

Figure 4 includes DSC curves of the MK-free renders with 10% of each type of PCM compared to their control render (CTRL-1). It is possible to clearly distinguish the melting process of each PCM after its addition to the lime-based mortars.

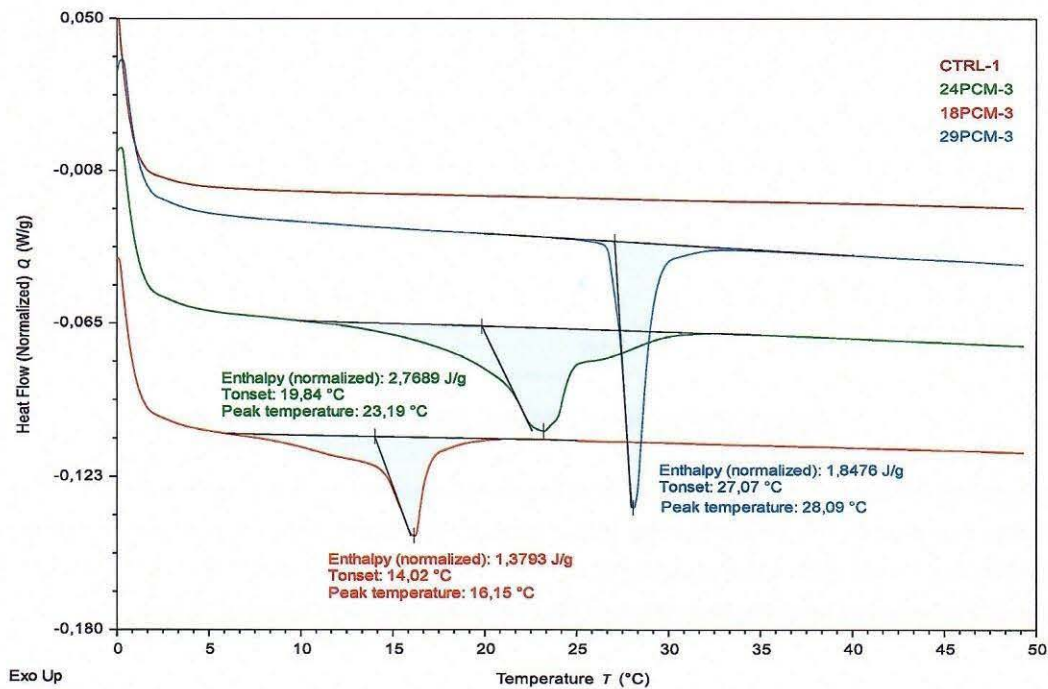


Figure 4. DSC curves of MK-free renders compared to CTRL-1.

The latent heat thermal energy storage capacity (measured as enthalpy) along with the onset temperatures and peak temperatures of PCM-bearing renders are included in Tables 4 and 5.

Table 4. ΔH_m , T_{peak} and T_{onset} values of PCM-free renders and 24PCM-renders.

Render	PCM (%)	Curing days	ΔH_m (J/g)	T_{peak} (°C)	T_{onset} (°C)
CTRL-1	0	28	0.0	-	-
	0	91	0.0	-	-
CTRL-2	0	28	0.0	-	-
	0	91	0.0	-	-
24PCM-1	5	28	0.74 ± 0.01	24.20 ± 0.01	19.80 ± 0.09
	5	91	0.83 ± 0.03	21.79 ± 0.09	19.68 ± 0.06
24PCM-2	5	28	0.84 ± 0.01	24.16 ± 0.01	16.43 ± 0.11
	5	91	0.92 ± 0.01	24.36 ± 0.01	16.73 ± 0.04
24PCM-3	10	28	2.78 ± 0.02	23.19 ± 0.01	19.80 ± 0.09
	10	91	2.13 ± 0.03	24.05 ± 0.02	19.68 ± 0.06

Continuation of Table 4. ΔH_m , T_{peak} and T_{onset} values of PCM-free renders and 24PCM-renders.

Render	PCM (%)	Curing days	ΔH_m (J/g)	T_{peak} (°C)	T_{onset} (°C)
24PCM-4	10	28	2.08 ± 0.01	23.51 ± 0.01	19.84 ± 0.08
	10	91	2.12 ± 0.02	24.23 ± 0.01	19.08 ± 0.04
24PCM-5	20	28	5.81 ± 0.01	23.87 ± 0.01	19.88 ± 0.09
	20	91	6.15 ± 0.01	24.18 ± 0.01	20.32 ± 0.08
24PCM-6	20	28	4.03 ± 0.02	23.89 ± 0.01	19.82 ± 0.09
	20	91	5.49 ± 0.02	24.18 ± 0.01	20.60 ± 0.07

Table 5. ΔH_m , T_{peak} and T_{onset} values of 18PCM-renders and 29PCM-renders.

Render	PCM (%)	Curing days	ΔH_m (J/g)	T_{peak} (°C)	T_{onset} (°C)
18PCM-1	5	28	0.83 ± 0.01	16.16 ± 0.01	14.18 ± 0.04
	5	91	0.42 ± 0.01	16.36 ± 0.01	13.80 ± 0.05
18PCM-2	5	28	0.62 ± 0.02	16.27 ± 0.01	14.31 ± 0.06
	5	91	0.41 ± 0.01	16.52 ± 0.01	14.54 ± 0.05
18PCM-3	10	28	1.38 ± 0.01	16.16 ± 0.01	13.97 ± 0.07
	10	91	1.52 ± 0.01	16.12 ± 0.01	13.67 ± 0.04
18PCM-4	10	28	1.33 ± 0.01	16.15 ± 0.01	13.92 ± 0.01
	10	91	1.63 ± 0.02	16.27 ± 0.01	14.06 ± 0.01
18PCM-5	20	28	4.41 ± 0.01	16.10 ± 0.01	13.66 ± 0.01
	20	91	3.18 ± 0.01	16.15 ± 0.01	13.76 ± 0.01
18PCM-6	20	28	2.53 ± 0.01	16.10 ± 0.01	13.72 ± 0.08
29PCM-1	5	28	0.92 ± 0.01	28.07 ± 0.03	27.08 ± 0.01
29PCM-2	5	28	1.17 ± 0.02	28.08 ± 0.01	27.05 ± 0.01
29PCM-3	10	28	1.84 ± 0.01	28.10 ± 0.01	27.07 ± 0.01
29PCM-4	10	28	1.24 ± 0.02	28.04 ± 0.01	27.05 ± 0.01
29PCM-5	20	28	4.80 ± 0.01	28.30 ± 0.01	27.15 ± 0.02
29PCM-6	20	28	4.99 ± 0.02	28.23 ± 0.01	26.93 ± 0.01

As expected, the capacity of the PCM-bearing mortars to store (or release) heat, as monitored by the enthalpy values, show an increasing pattern as the amount of PCM incorporated in the mortar increases (Figure 5). This pattern is maintained in both curing ages and after the addition of MK. In general, MK-free renders show higher enthalpy values and therefore heat storage capacity, this is particularly true for high percentages of PCM.

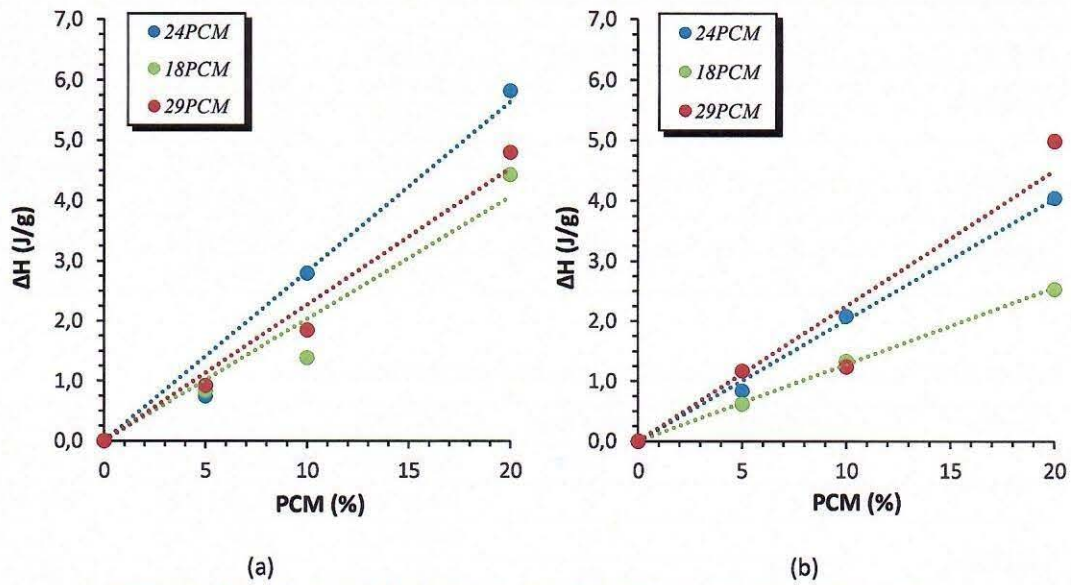


Figure 5. Enthalpy values of renders at 28 curing days: (a) MK-free; (b) 20% MK.

Regarding the C_p measurements (that is, the sensible heat capacity), it was observed that the addition of the PCMs does not affect severely the C_p of the render either when the PCM is in the solid phase or when it is in the liquid phase (Figures 6-7) (that is, excluding the temperature interval in which a phase change – melting or solidification - takes place). In the case of PCM-bearing mortars, the thermodynamic melting process is clearly observed in where the C_p values vary drastically (Figures 6-7). The C_p values obtained in all cases are within the usual range for these materials (0.73-1.26 J/g°C) [6,7]. However, in this work, there was not a clear trend to increase the heat capacity of the material when PCMs were incorporated [6,7].

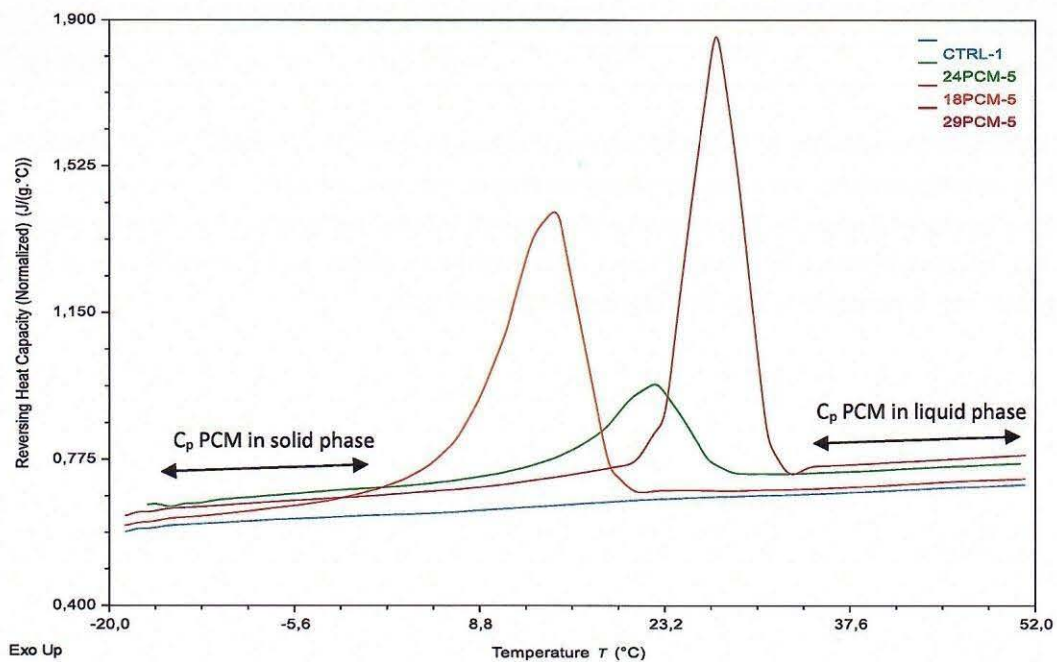


Figure 6. C_p values of MK free renders at 28 curing days.

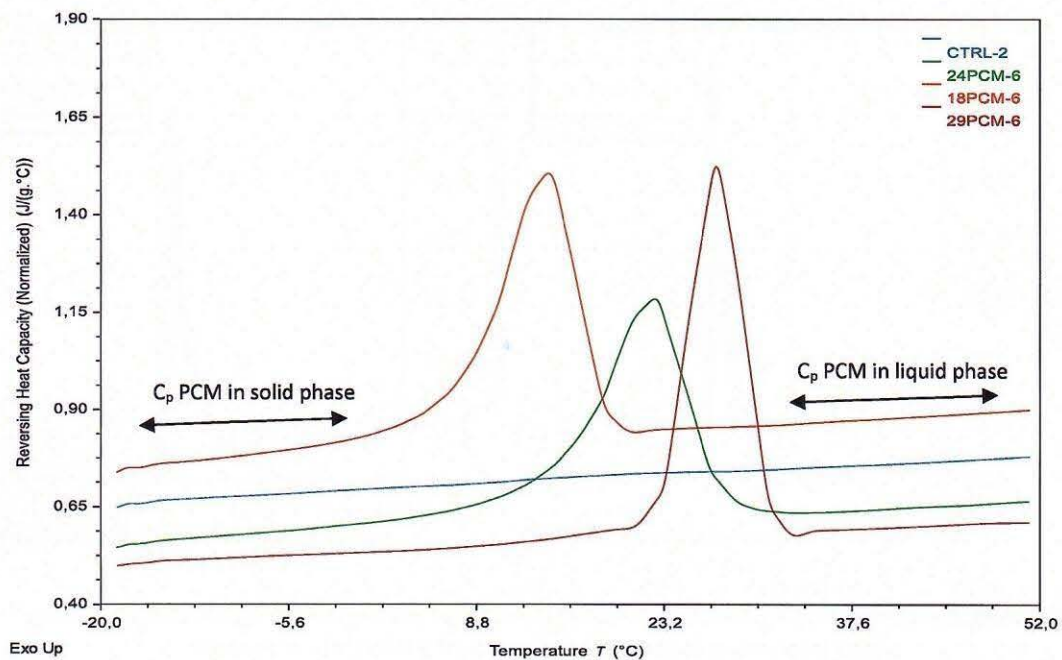


Figure 7. C_p values of 20% MK renders at 28 curing days.

3.2 Thermal conductivity measurements

Tables 3-5 include thermal conductivity coefficient (λ) values of the lime renders measured at 5°C, 15°C, 25°C and 35°C. Thermal conductivity is the rate at which heat flows through a material. Therefore, the higher the thermal conductivity coefficient (λ), the higher the thermal conductivity of the material.

The λ values obtained in all cases are within the usual range for these materials [6,7]. It is observed in PCM-free renders that the presence of metakaolin does not affect the thermal conductivity of the samples. In addition, PCMs apparently do not have a strong influence on the thermal conductivity either. These values are consistent with the pore size distributions as the addition of PCMs had little effect on the pore size distributions (Figure 8) due to the previous optimization of the mix compositions by using appropriate chemical additives. As it can be seen, main pore size and critical pore size (threshold for the main Hg intrusion) are kept almost constant for the different renders. However, some previous works [6,7] reported a decrease in thermal conductivity after the addition of PCM ascribing it to the lower conductivity of this additive. This fact might be ascribed to the fact that in those works, conversely to the current one, the percentage of mixing water to achieve adequate workability was adjusted having probably strong influence in the macroscopic structure of the material. In this work the water ratio remained constant in all renders resulting in tiny differences in the structure of the renders and therefore in their thermal conductivity (Tables 6-8).

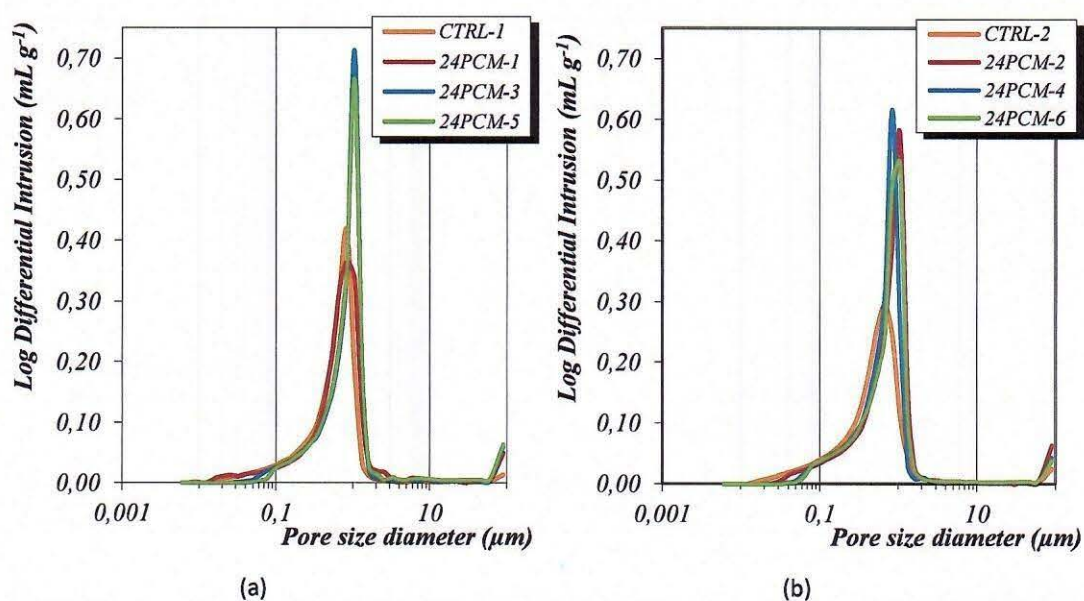


Figure 8. Comparison of pore size distribution of (a) MK-free renders containing 24PCM at 91 curing days; (b) Renders containing 24PCM and 20% MK at 91 curing days.

The maintenance of the thermal conductivity of the renders after the incorporation of the additives could be advantageous to achieve maximum heat storage. In this sense, the matrix of the rendering mortar should be able to allow the heat to reach the inner part of the microencapsulated PCMs, to undergo the phase change and thus be able to regulate moderately the temperature.

Table 6. Thermal conductivity coefficients of PCM-free renders at different temperatures.

PCM-free		
	0% MK	20% MK
T (°C)	λ (W/ m·K)	λ (W/ m·K)
5	0.37 ± 0.05	0.38 ± 0.03
15	0.37 ± 0.05	0.38 ± 0.03
25	0.37 ± 0.05	0.38 ± 0.03
35	0.37 ± 0.05	0.38 ± 0.03

Table 7. Thermal conductivity coefficients of 24PCM renders at different temperatures.

24PCM						
	5% PCM		10% PCM		20% PCM	
	0% MK	20% MK	0% MK	20% MK	0% MK	20% MK
T (°C)	λ (W/ m·K)	λ (W/ m·K)	λ (W/ m·K)	λ (W/ m·K)	λ (W/ m·K)	λ (W/ m·K)
5	0.44 ± 0.04	0.36 ± 0.03	0.40 ± 0.03	0.39 ± 0.05	0.36 ± 0.06	0.38 ± 0.01
15	0.45 ± 0.04	0.36 ± 0.03	0.40 ± 0.03	0.39 ± 0.04	0.36 ± 0.06	0.38 ± 0.01
25	0.45 ± 0.05	0.35 ± 0.03	0.40 ± 0.03	0.40 ± 0.03	0.37 ± 0.06	0.38 ± 0.01
35	0.45 ± 0.05	0.35 ± 0.04	0.40 ± 0.04	0.40 ± 0.03	0.37 ± 0.06	0.38 ± 0.01

Table 8. Thermal conductivity coefficients of 18PCM renders at different temperatures.

T (°C)	18PCM					
	5% PCM		10% PCM		20% PCM	
	0% MK	20%MK	0% MK	20%MK	0% MK	20%MK
λ (W/ m·K)	λ (W/ m·K)	λ (W/ m·K)	λ (W/ m·K)	λ (W/ m·K)	λ (W/ m·K)	
5	0.39 ± 0.02	0.40 ± 0.02	0.40 ± 0.08	0.41 ± 0.01	0.46 ± 0.02	0.37 ± 0.08
15	0.39 ± 0.02	0.40 ± 0.02	0.41 ± 0.08	0.41 ± 0.01	0.46 ± 0.02	0.38 ± 0.08
25	0.39 ± 0.02	0.40 ± 0.02	0.41 ± 0.08	0.40 ± 0.01	0.46 ± 0.02	0.38 ± 0.08
35	0.39 ± 0.02	0.40 ± 0.02	0.40 ± 0.08	0.40 ± 0.01	0.45 ± 0.02	0.38 ± 0.08

4 Conclusions

Thermal performance of PCM-enhanced air lime renders was studied. The specific heat C_p , the enthalpy ΔH ascribed to the phase change and the melting temperature of the PCMs were determined by Differential Scanning Calorimetry (DSC). Results showed that C_p values barely vary with the percentage of PCM. As expected, the latent heat thermal energy storage capacity (measured as enthalpy) values ascribed to the melting process of the PCMs added to the renders show an almost linear trend, the higher the amount of this additive, the higher the enthalpy.

Thermal conductivity measurements have shown that the addition of PCMs does not weaken the thermal conductivity of the renders. This could be due to the optimization of the mix composition during the mortar preparation, in which the percentage of mixing water is remained constant resulting in little variation in the macrostructure of the material.

Favourable results have proven the effect of these PCMs on the thermal performance of the renders offering promise for improved thermal efficiency of Cultural Heritage building materials. The capacity of the renders to store/release heat demonstrated at a laboratory scale and the use of models that imitate building envelopes might be also suggested as future achievements.

Acknowledgements

Funded by Ministerio de Ciencia e Innovación, grant number PID2020-119975RB-I00 LIMORTHER.

References

- [1] Frigione, M.; Lettieri, M.; Sarcinella, A.; Barroso de Aguiar, J. Sustainable polymer-based Phase Change Materials for energy efficiency in buildings and their application in aerial lime mortars. *Constr Build Mater* 2020, 231.
- [2] Himran, S.; Suwono, A.; Mansoor, G.A. Characterization of alkanes and paraffin waxes for application as phase change energy storage medium. *Energy Sources* 1994,16, pp. 117–28.
- [3] Liu, H.; Wang, X.; Wu, D. Innovative design of microencapsulated phase change materials for thermal energy storage and versatile applications: A review. *Sustain Energy Fuels* 2019, 3, pp. 1091–149.

- [4] Farid, MM.; Khudhair, A.M.; Razack, S.A.K.; Al-Hallaj, S. A review on phase change energy storage: Materials and applications. *Energy Convers Manag* 2004, 45 pp. 1597–615.
- [5] Ukrainczyk, N.; Kurajica, S.; Šipušić, J. Thermophysical comparison of five commercial paraffin waxes as latent heat storage materials. *Chem Biochem Eng Q* 2010, 24, pp. 129–37.
- [6] Theodoridou, M.; Kyriakou, L.; Ioannou, I. PCM-enhanced Lime Plasters for Vernacular and Contemporary Architecture. *Energy Procedia* 2016, 97, pp. 539–45.
- [7] Haurie, L.; Serrano, S.; Bosch, M.; Fernandez, A.I.; Cabeza, L.F. Single layer mortars with microencapsulated PCM: Study of physical and thermal properties and fire behaviour. *Energy Build* 2016, 111, pp. 393–400.
- [8] García-Viñuales, S.; Rubio, C.; Martínez-Izquierdo, L.; Zornoza, B.; Piera, E.; Caballero, M.A.; Téllez, C. Study of Melamine-Formaldehyde / Phase Change Material Microcapsules for the Preparation of Polymer Films by Extrusion. *Membranes* 2022, 12.
- [9] Lanas, J.; Sirera, R.; Alvarez, J.I. Compositional changes in lime-based mortars exposed to different environments. *Thermochim Acta* 2005, 429, pp. 219–26.